NATIONAL AERONAUTICS AND SPACE ADMINISTRATION

MSC INTERNAL NOTE NO. 69-FM-63

March 17, 1969

EVALUATION OF STEEP FINAL APPROACH PHASE LUNAR DESCENT TRAJECTORIES

Advanced Mission Design Branch

MISSION PLANNING AND ANALYSIS DIVISION

MANNED SPACECRAFT CENTER
HOUSTON, TEXAS

MSC INTERNAL NOTE NO. 69-FM-63

EVALUATION OF STEEP FINAL APPROACH PHASE LUNAR DESCENT TRAJECTORIES

By John T. McNeely
Advanced Mission Design Branch

March 17, 1969

MISSION PLANNING AND ANALYSIS DIVISION
NATIONAL AERONAUTICS AND SPACE ADMINISTRATION
MANNED SPACECRAFT CENTER
HOUSTON, TEXAS

Approved: James P. Taylor for
Jack Funk, Chief
Advanced Mission Design Branch

Approved:
John P. Mayer, Chief
Mission Planning and Analysis Division

FIGURES

Figure		Page
1	Force vector diagrams for vehicle in final approach phase of lunar descent (constant flight-path angle)	
	(a) Vehicle at arbitrary position along descent trajectory	15
	(b) Indication of pitch angle ($\alpha + \gamma$) necessary to maintain constant γ approach	15
2	Force vector diagram for vehicle in abort phase after high gate	16
3	Variation in the velocity at high gate with flight-path angle and thrust	17
4	Characteristic velocity required from high gate to low gate	18
5	Gravity losses incurred from high gate to low gate	19
6	Variation in LM weight at high gate with flight-path angle and thrust	20
7	Variation in thrust angle at high gate with flight-path angle and thrust	21
8	Variation in ground range from high gate to landing site with flight-path angle	22
9	Variation in pullout altitude with time of abort initiation and flight-path angle	23
10	Abort pullout capability of the LM ascent stage	24
11	Method of abort from steep descent	25
12	Characteristic velocity required to attain 60 000-foot by 30 000-nautical mile orbit . . .	26

Figure		Page
13	Characteristic velocity required for LM abort during a 30° flight-path angle final approach phase	27
14	Characteristic velocity required for LM abort during a 45° flight-path angle final approach phase	28
15	Characteristic velocity required for LM abort during a 60° flight-path angle final approach phase	29
16	Characteristic velocity required for abort during a 75° flight-path angle final approach phase	30
17	Total ΔV required for LM descent using a steep final approach phase	31
18	Low-gate offset technique for landing site visibility	32
19	Low-gate offset technique required for landing site visibility at high gate	33
20	Look angle with low-gate offset	34

EVALUATION OF STEEP FINAL APPROACH PHASE LUNAR DESCENT TRAJECTORIES

By John T. McNeely

SUMMARY

Problems of descent, abort, and landing site visibility during steep final approach phase lunar descent trajectories have been studied. The equations of motion were derived in closed form and have been programed for a vehicle on a constant flight-path angle trajectory and for a vehicle which aborts from this trajectory to a constant thrust pitch angle trajectory. The conditions desired at low gate are the input quantities for the descent program, and the conditions existing at the time of abort are the input quantities for the abort program. Data are presented which show the effect of descent flight-path angles of up to 90°. Abort data for these trajectories are also presented.

For an abort trajectory as well as for a descent trajectory, it appears feasible to have a descent flight-path angle as large as 55° for the final approach phase of a lunar landing mission provided that the CSM delivers the LM to a 50 000-foot altitude circular orbit. This upper limit on flight-path angle drops to approximately 31° if the LM descends from a 60-n. mi. altitude circular orbit. However, a dispersion analysis has not been conducted and is beyond the scope of this study.

INTRODUCTION

Post-Apollo lunar landing missions may require steep lunar descent trajectories if lunar landing sites are chosen which have very rough surrounding terrain or which are in craters such as Copernicus, Abulfeda or Aristarchus. The steep descent trajectories reduce LM landing radar problems over rough terrain and may increase accessibility by opening the lighting window.

To determine the feasibility of a steep final approach phase descent trajectory, equations of motion have been derived and programed

for the descent and abort phases. A parametric scan of the descent trajectories was made to determine their general characteristics. Maximum acceptable descent flight-path angles which satisfied the abort criteria were determined. Finally, characteristics of these maximum flight-path angle trajectories and landing site visibility problems were investigated.

SYMBOLS

C_N	constant of integration, N = 1, ..., 8
F_X	force in X direction
F_Z	force in Z direction
g	gravity at surface of moon, 5.3235 ft/sec^2
H	altitude at end of final approach phase
I_{sp}	specific impulse
M	mass of vehicle
M_o	mass at end of final approach phase
M_1	initial weight of LM ascent stage
$\dot{M}$	fuel mass flow rate
t	time
T	thrust
V	velocity at end of final approach phase
X	position along X-axis, horizontal
$\dot{X}$	velocity in X direction
$\ddot{X}$	acceleration in X direction
Z	position along Z-axis, vertical
$\dot{Z}$	velocity in Z direction

$\ddot{Z}$	acceleration in Z direction
α	thrust pitch angle measured from flight-path angle, descent phase
ϕ	sum of thrust pitch angle and flight-path angle, $\alpha + \gamma$
γ	flight-path angle measured from horizontal
θ	thrust pitch angle measured from vertical, abort phase
V_Z	velocity in Z direction at time of abort
V_X	velocity in X direction at time of abort
Z_Z	position along Z-axis at time of abort
X_X	position along X-axis at time of abort

ANALYSIS

Derivation of Descent Equations of Motion

The program which has been developed for a vehicle on a constant flight-path angle trajectory during the final approach phase determines the vehicle velocity, position, weight, and attitude as a function of time. The desired vehicle and trajectory characteristics at low gate are input quantities. A flat moon and a constant gravitational potential were assumed and are reasonable assumptions for small altitude changes and short ranges. The problem was further simplified by the assumption of a two-dimensional trajectory. Thrust was considered to be constant throughout this phase.

A free-body diagram which shows the vehicle at some arbitrary position along the descent trajectory is presented in figure 1(a). Summation of forces in the vertical (Z) and horizontal (X) directions results in

$$F_Z = T \sin \phi - Mg \tag{1}$$

$$F_X = T \cos \phi \tag{2}$$

The acceleration in the Z and X directions is found from

$$\ddot{Z} = \frac{T}{M} \sin \phi - g \tag{3}$$

$$\ddot{X} = \frac{T}{M} \cos \phi \tag{4}$$

The angle ϕ is the angle measured from the horizontal to the thrust vector. Because mass changes as fuel is used, ϕ must also change to maintain a constant flight-path angle. A force vector diagram that shows the pitch angle α necessary to obtain the flight-path angle γ is presented in figure 1(b). The angle ϕ is

$$\phi = \gamma + \alpha \tag{5}$$

From figure 1(b), note that

$$Mg \cos \gamma = T \sin \alpha \tag{6}$$

or

$$\alpha = \sin^{-1} \left[\frac{Mg}{T} \cos \gamma \right] \tag{7}$$

Substitution of equations 5 and 7 into equations 3 and 4 results in

$$\ddot{Z} = \frac{T}{M} \sin \left[\gamma + \sin^{-1} \left(\frac{Mg}{T} \cos \gamma \right) \right] - g \tag{8}$$

$$\ddot{X} = \frac{T}{M} \cos \left[\gamma + \sin^{-1} \left(\frac{Mg}{T} \cos \gamma \right) \right] \tag{9}$$

Trigonometric substitution of the sum of two angles into equations (8) and (9) gives

$$\ddot{Z} = \frac{T}{M} \left\{ \sin \gamma \cos \left[\sin^{-1} \left(\frac{Mg}{T} \cos \gamma \right) \right] + \cos \gamma \sin \left[\sin^{-1} \left(\frac{Mg}{T} \cos \gamma \right) \right] \right\} - g \tag{10}$$

$$\ddot{X} = \frac{T}{M} \left\{ \cos \gamma \cos \left[\sin^{-1} \left(\frac{Mg}{T} \cos \gamma \right) \right] - \sin \gamma \sin \left[\sin^{-1} \left(\frac{Mg}{T} \cos \gamma \right) \right] \right\} \tag{11}$$

After the substitutions have been made for the sine and cosine of an inverse trigonometric function, the acceleration of the vehicle is obtained from

$$\ddot{Z} = \frac{T \sin \gamma}{M} \sqrt{1 - u^2} - g \sin^2 \gamma \tag{12}$$

$$\ddot{X} = \frac{T \cos \gamma}{M} \sqrt{1 - u^2} - g \sin \gamma \cos \gamma \tag{13}$$

where

$$M = M_o + \dot{M}t \tag{14}$$

$$\dot{M} = \frac{T}{I_{sp}} \tag{15}$$

$$u = \frac{Mg}{T} \cos \gamma \tag{16}$$

The term $\dot{M}t$ in equation (14) is positive because the problem is solved in reverse order and because fuel is added to the vehicle as time increases. Integration of these equations yields the two components of velocity.

$$\dot{Z} = \frac{T \sin \gamma}{\dot{M}} \left[\sqrt{1 - u^2} - \log \left(\frac{1 + \sqrt{1 - u^2}}{u} \right) \right] - gt \sin^2 \gamma + C_3 \tag{17}$$

$$\dot{X} = \frac{T \cos \gamma}{\dot{M}} \left[\sqrt{1 - u^2} - \log \left(\frac{1 + \sqrt{1 - u^2}}{u} \right) \right] - gt \sin \gamma \cos \gamma + C_1 \tag{18}$$

where

$$C_1 = V \cos \gamma - \frac{T \cos \gamma}{\dot{M}} \sqrt{1 - D^2 M_o^2} + \frac{T \cos \gamma}{\dot{M}} \log \left[\frac{1 + \sqrt{1 - D^2 M_o^2}}{DM_o} \right] \tag{19}$$

$$C_3 = V \sin \gamma - \frac{T \sin \gamma}{\dot{M}} \sqrt{1 - D^2 M_o^2} + \frac{T \sin \gamma}{\dot{M}} \log \left[\frac{1 + \sqrt{1 - D^2 M_o^2}}{DM_o} \right] \tag{20}$$

$$D = \frac{g \cos \gamma}{T} \tag{21}$$

Integration of equations (17) and (18) gives the position of the vehicle as a function of time.

$$Z = \frac{T \sin \gamma}{2D\dot{M}^2} \left[u \sqrt{1 - u^2} - \sin^{-1} u \right] - \frac{Tu \sin \gamma \cosh^{-1} \frac{1}{u}}{D\dot{M}^2} - \frac{gt^2 \sin^2 \gamma}{2} + C_3 t + C_4 \tag{22}$$

$$X = \frac{T \cos \gamma}{2D \dot{M}^2} \left[u\sqrt{1 - u^2} - \sin^{-1} u \right] - \frac{Tu \cos \gamma \cosh^{-1} \frac{1}{u}}{D\dot{M}^2} \tag{23}$$

$$- \frac{gt^2 \cos \gamma \sin \gamma}{2} + C_1 t + C_2$$

where

$$C_2 = - \frac{T \cos \gamma}{2D \dot{M}^2} \left[DM_o \sqrt{1 - D^2 M_o^2} - \sin^{-1} (DM_o) \right] \tag{24}$$

$$+ \frac{T \cos \gamma}{\dot{M}^2} \left[M_o \cosh^{-1} \left(\frac{1}{DM_o} \right) \right]$$

$$C_4 = H - \frac{T \sin \gamma}{2D \dot{M}^2} \left[DM_o \sqrt{1 - D^2 M_o^2} - \sin^{-1} (DM_o) \right] \tag{25}$$

$$+ \frac{T \sin \gamma}{\dot{M}^2} \left[M_o \cosh^{-1} \left(\frac{1}{DM_o} \right) \right]$$

If the conditions at a certain altitude (e.g., high gate) are desired, a simple iteration can be performed and the time corresponding to the desired altitude obtained from equation (22); then other equations can be solved by use of the correct time.

Derivation of Abort Equations of Motion

An abort during the final approach phase of a lunar descent trajectory by use of the ascent stage may become necessary. The program which has been developed for a vehicle on a constant thrust pitch angle trajectory during an abort from the final approach phase determines the vehicle velocity, position, and weight as a function of time. The conditions at the time of abort are input quantities which can be obtained from the equations presented in the preceding section. The equations which govern the abort trajectory are derived in this section for a constant thrust pitch angle θ, measured from the vertical. A force vector diagram for the vehicle at some arbitrary position along the abort trajectory is presented in figure 2. Summation of forces in the vertical (Z) and horizontal (X) direction yields

$$F_Z = T \cos \theta - Mg \tag{26}$$

$$F_X = T \sin \theta \tag{27}$$

The acceleration in the Z and X directions then can be found from

$$\ddot{Z} = \frac{T}{M} \cos \theta - g \tag{28}$$

$$\ddot{X} = \frac{T}{M} \sin \theta \tag{29}$$

Integration of these equations yields the velocity components

$$\dot{Z} = \frac{T \cos \theta \log M}{\dot{M}} - gt + C_5 \tag{30}$$

and

$$\dot{X} = \frac{T \sin \theta \log M}{\dot{M}} + C_7 \tag{31}$$

where

$$C_5 = V_Z - \frac{T \cos \theta \log M_1}{\dot{M}} \tag{32}$$

$$C_7 = V_X - \frac{T \sin \theta \log M_1}{\dot{M}} \tag{33}$$

Integration of equations (30) and (31) gives the position of the vehicle as a function of time after abort.

$$Z = \frac{T \cos \theta}{\dot{M}^2} [M \log (M) - M] - \frac{gt^2}{2} + C_5 t + C_6 \tag{34}$$

$$X = \frac{T \sin \theta}{\dot{M}^2} [M \log (M) - M] + C_7 t + C_8 \tag{35}$$

where

$$C_6 = Z_Z - \frac{T \cos \theta}{\dot{M}^2} \left[M_1 \log (M_1) - M_1 \right] \tag{36}$$

$$C_8 = X_X - \frac{T \sin \theta}{\dot{M}^2} \left[M_1 \log (M_1) - M_1 \right] \tag{37}$$

$$M = M_1 + \dot{M}t \tag{38}$$

In this case, fuel is being subtracted as time increases; therefore, the term $\dot{M}t$ in equation (38) is negative. The position X is measured from the original point of low gate on the descent trajectory, positive in the direction of high gate. The time of pull-up (when $\dot{Z} = 0$) can be found by a simple iteration of equation (30). The position then can be found from equations (34) and (35).

PROGRAM APPLICATION

Vehicle Description

The data that were generated to illustrate the output of the two programs described in this report use the characteristics of the extended LM (ELM) as the descent vehicle. The characteristics of this vehicle were obtained from references 1, 2, and 3 and are summarized in table I. The weight at low gate is an input quantity for the descent program and has a nominal value of 18 265 pounds. This nominal value allows a ΔV of 667 fps for the landing phase (descent from 500 ft plus 50 sec of hover) and gives a nominal propellant weight of 339 pounds for dispersions. A maximum descent stage thrust of 10 500 pounds was used with variations in I_{sp} of 288.5 seconds for 10 percent thrust to 301.7 seconds for maximum thrust.

Descent Final Approach Phase Parametric Scan

A parametric scan is presented in figures 3 through 8 which shows the effect of steep descent angles on the final approach phase descent trajectory. In all cases, the altitudes at high gate and low gate are 10 000 feet and 500 feet, respectively. The velocity and weight at low gate are 0 fps and 18 265 pounds, respectively. The variation in the velocity at high gate is shown in figure 3 as a function of flight-path angle and thrust during the final approach phase of lunar descent. The characteristic velocity (V_c) required from high gate to low gate is shown in figure 4 as a function of flight-path angle and thrust, and the corresponding gravity losses are shown in figure 5. For any given flight-path angle, a minimum characteristic velocity occurs between the thrust levels of 4900 and 6200 pounds. This situation occurs only during the final approach phase of lunar descent. When the braking phase (50 000 ft to high gate) is considered in conjunction with the data in figure 4, the shape of the curves will change, and the steeper descent trajectories will have the higher ΔV requirements.

The variation in vehicle weight at high gate as a function of thrust and flight-path angle during the final approach phase is seen in figure 6. As with the characteristic velocity, a minimum value for the weight at high gate exists for each given flight-path angle and thrust level between 4900 and 6200 pounds.

The thrust angle measured from the horizontal is shown in figure 7 as a function of thrust and flight-path angle γ. As expected for low values of thrust and γ, a significant portion of the thrust vector is required to stop vertical descent. The ground range from high gate to the landing site is shown in figure 8 as a function of flight-path angle. One of the real advantages of the steep descent angle approach is that only a small range is required. This small range reduces the LM landing radar problems over rough terrain by allowing for a longer observation of the landing site area by the radar.

Abort from the Descent Trajectory

As an example of how the descent and abort programs discussed in this report can be used, the landing and abort performance problems of an ELM have been considered. The characteristics of this LM were given in the preceding section, and many trade-offs were seen to exist between flight-path angle and thrust. The problems are not associated with the steep descent trajectory, but rather with the abort from this trajectory. For that reason, the abort problem is considered first.

When the descent flight-path angle and descent thrust are both large, vertical velocity as a function of altitude is also relatively large. Abort from these trajectories with the LM ascent stage is impossible because of the reduced thrust-to-weight ratio of this stage. The problem easily is seen in figure 9 which shows pullout altitude as a function of time after high gate of abort initiation. The descent stage thrust level is 6000 pounds. A descent flight-path angle γ of approximately 46° results in a pullout at the lunar surface if abort is initiated 35 seconds after high gate. Abort is not possible during the entire final approach phase trajectory if γ is greater than 46° because aborts during certain portions of this trajectory (dead man zones) result in a pullout below the lunar surface. By reduction of the descent stage thrust, dead man zones can be eliminated for all descent flight-path angles. The minimum altitude at pullout is shown in figure 10 as a function of descent flight-path angle and descent stage thrust. A descent flight-path angle of 90° requires the lowest thrust level (5710 lb) to eliminate dead man zones. If the thrust is reduced to 4945 pounds, the minimum altitude at pullout is 300 feet. The thrust level that corresponds to a

minimum altitude of 300 feet at pullout for any given flight-path angle is labeled in figure 10 and is the thrust level used for the rest of this example case.

The previous analysis dealt only with the problem of stopping vertical descent before the lunar surface is reached. A second problem associated with abort is the achievement of a safe orbit after vertical descent is stopped. A schematic that presents data for the solution of the abort problem in two phases is given in figure 11. The descent stage was assumed to be jettisoned with a 3-second delay between DPS shutdown and APS thrust buildup. The constant thrust pitch angle abort program described in this report then was used to determine the ascent stage position and velocity as a function of time until vertical descent was stopped (point B in fig. 11). The ΔV required to attain a safe orbit from point B of 60 000 feet by 30 n. mi. was obtained from reference 4. The ΔV data are very insensitive to the vehicle altitude at point B and were calculated by use of an optimum pitch profile program. These data are shown in figure 12 as a function of the horizontal velocity of the vehicle at point B.

The total ΔV required to abort successfully from a steep descent trajectory was computed by use of the previously described method of solution and is shown in figures 13 through 16. Descent flight-path angles of 30°, 45°, 60°, and 75° are considered. In each of the figures, the solid lines are constant time lines that indicate the time of abort initiation after high gate. The dashed lines are constant altitude lines that correspond to the altitude at pullout (closest approach to the lunar surface). A descent stage thrust was chosen for each descent flight-path angle γ so that the minimum pullout altitude for any abort is 300 feet. For a pullout altitude of 300 feet, the maximum ΔV required for abort is 5985 fps for a γ of 30°, 6019 fps for a γ of 45°, 6110 fps for a γ of 60°, and 6186 fps for a γ of 75°.

The ΔV requirements for abort increase as the pullout altitude increases (figs. 13 through 16). Although altitude requirements are not explicitly defined, abort at higher altitudes will probably dictate a relatively high pullout altitude because of the possible magnitude of the unknown altitude error at that time. As the vehicle approaches the lunar surface, radar updates should make it possible to use a lower pullout altitude. Depending on the constraints and the maximum ΔV capability of the LM ascent stage, it appears possible to abort from a descent trajectory that has a γ as large as 50° to 60°. For an abort to be successful, steeper descent trajectories would required a reduction in the descent stage thrust from that used for the example problem.

The Descent Trajectory

In previous sections a parametric scan was made of the final approach phase descent trajectory. The final approach phase abort problem then was solved to determine the specific area of interest for the descent stage thrust level. Thrust was chosen as a function of the descent flight-path angle γ so that the minimum pullout altitude for any abort was 300 feet. The conditions at high gate were determined, and data for the braking phase, which match the conditions at high gate, were obtained from the Landing Analysis Branch, MPAD. By use of these data, the total ΔV required for descent from a 50 000-foot circular orbit to landing was obtained and is shown in figure 17 as a function of the flight-path angle during the final approach phase. The total ΔV varies from 6790 fps for a γ of 25° to 7160 fps for a γ of 90°. These values are based on a landed LM weight of 17 044 pounds, which corresponds to a fully fueled LM separation weight of 34 272 pounds. A ΔV of 6997 fps is budgeted in Apollo for the descent trajectory, based on a LM separation weight of 33 500 pounds. This ΔV allowance, which is almost the maximum ΔV capability of the LM descent stage, crosses the curve in figure 17 at a γ of approximately 55°. This value for γ is in the area of the upper limit on γ for an abort as well.

LANDING SITE VISIBILITY

One of the problems associated with the steep descent trajectory is landing site visibility. It has been assumed in the foregoing analysis that the vehicle velocity at low gate is zero and that the landing site is directly below low gate. When these conditions exist, the landing site will not appear 5° above the window edge at any time during the constant γ final approach phase. A solution for this problem is to offset low gate so that the landing site can be seen and then to fly some modified trajectory. A schematic of one such modified trajectory is shown in figure 18. The method is shown only to indicate a possible technique. No attempt was made to optimize the ΔV cost in this example, which employs a descent flight-path angle of 45°. If low gate is offset 2126 feet from the landing site, the site can be seen 5° above the window edge at high gate and higher above the window edge as the vehicle approaches low gate. The flight-path angle is held at 45° and the thrust at 5300 pounds until an altitude of 1705 feet is reached. The thrust then is reduced to 4961 pounds, and the pitch angle is increased to 90° (vertical). At an altitude of 500 feet, vertical descent stops and the landing site is approximately 500 feet away. The horizontal velocity then is reduced to zero by a thrust of 6500 pounds at a pitch angle of approximately 30°. This trajectory costs approximately 83 fps more than a constant γ approach

all the way to low-gate. This ΔV represents slightly more than 15 seconds of hover time. When this method is used, the landing site can be seen well above the window edge during all of the final approach phase except for the last few seconds.

The amount that low gate must be offset so that the landing site can be seen at high gate is shown in figure 19 as a function of the flight-path angle γ during the final approach phase. The amount of offset varies from 1750 feet for a γ of 35° to 5774 feet for a γ of 90°. The result of this offset can be seen in figure 20 which shows look angle as a function of time to go to low gate and of flight-path angle. A look angle of 30° corresponds to the visibility of the landing site 5° above the window edge. These data were calculated with a constant γ trajectory assumed all the way to low gate. A pitch-up maneuver near low gate yields an even greater look angle. The look angle for a typical Apollo descent (one phase) is shown in figure 20 for comparison purposes. Low gate offset permits landing site visibility for the constant γ approach to compare favorably with the visibility for an Apollo descent trajectory.

CONCLUSIONS

A technique has been presented for analysis of the effects of steep descent angle on the final approach phase of a lunar landing mission. Equations for the vehicle velocity, position, weight, and attitude are given as functions of time in closed form. Closed form solutions which give the characteristics of abort trajectories as functions of time are also presented. In both descent and abort techniques, a flat moon, a constant gravitational potential, a two-dimensional trajectory, and constant thrust are assumed. With this model, steep final approach phase descent trajectories are evaluated with the following constraints.

1. The CSM delivers the LM to a 50 000-foot altitude circular orbit.

2. The altitudes at high gate and low gate are 10 000 feet and 500 feet, respectively, and the velocity at low gate is zero.

3. The descent stage thrust is specified as a function of γ such that the minimum pullout altitude for any abort is 300 feet (fig. 10).

4. The minimum acceptable orbit for an abort maneuver is 60 000 feet by 30 n. mi.

The conclusions of the analysis are the following.

1. It is possible to have a descent flight-path angle of as large as 55° and not exceed the ΔV which is currently budgeted in Apollo for LM descent.

2. If the CSM cannot deliver the LM to a circular orbit lower than 60-n. mi. altitude, the 55° upper limit on γ drops to approximately 31°. A dispersion analysis has not been conducted and is beyond the scope of this paper.

3. If the descent flight-path angle is less than approximately 55°, abort from the descent trajectory to a 60 000-foot by 30-n. mi. altitude orbit can be successfully accomplished with the LM ascent stage.

4. The problem of landing site visibility for a constant γ approach can be solved by low-gate offset.

TABLE I.- CHARACTERISTICS OF ASCENT AND DESCENT STAGES

OF THE EXTENDED LM

Maximum total weight for both stages, lb	34 272
Maximum usable fuel for the descent stage, lb	17 588
Nominal fuel used for descent, lb	17 228
Nominal weight at landing, lb	17 044
Fuel allowance for landing phase (667 fps), lb	1 221
Nominal weight at low gate (500 ft), lb	18 265
Descent stage	
Maximum thrust, lb	10 500
I_{sp} at 10% thrust, sec	288.5
I_{sp} at 25% thrust, sec	292.5
I_{sp} at 50% thrust, sec	295.8
I_{sp} at 60% thrust, sec	300.6
I_{sp} at 65% thrust, sec	301.6
I_{sp} at FTP, sec	301.7
Ascent stage	
Thrust, lb	3 627
I_{sp}, sec	303.4

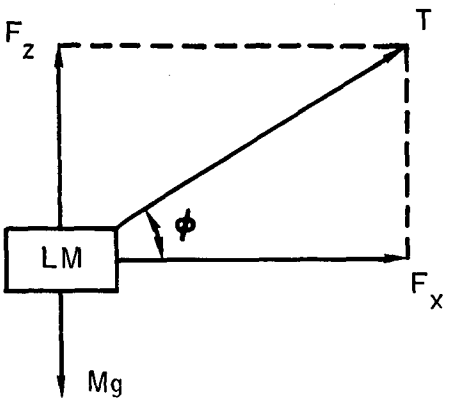

(a) Vehicle at arbitrary position along descent trajectory.

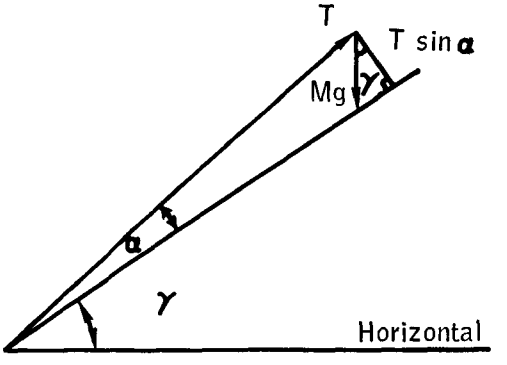

(b) Indication of pitch angle $(\alpha+\gamma)$ necessary to maintain constant γ approach.

Figure 1.- Force vector diagrams for vehicle in final approach phase of lunar descent (constant flight-path angle).

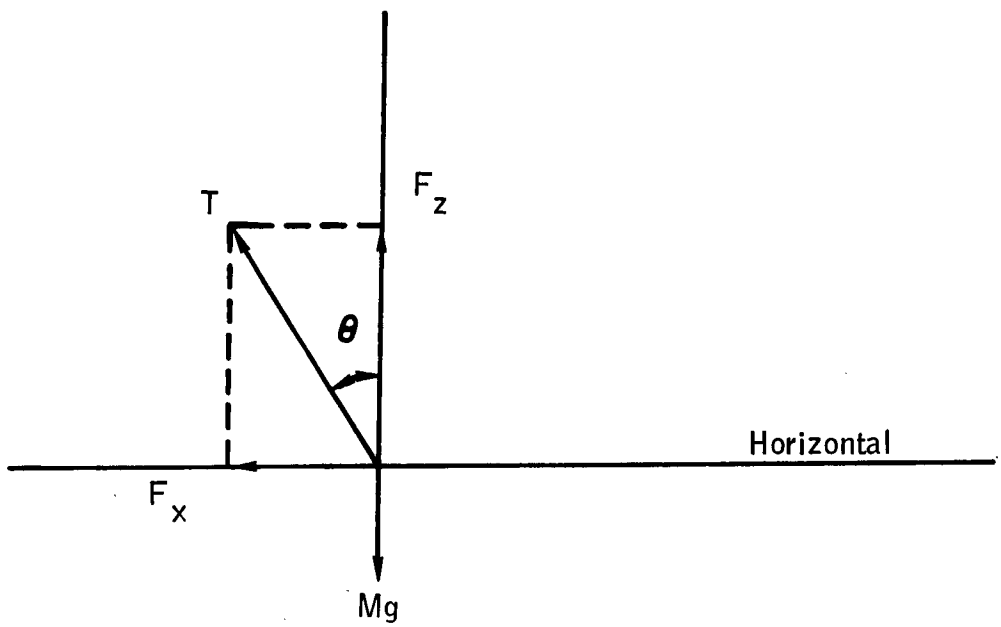

Figure 2.- Force vector diagram for vehicle in abort phase after high gate.

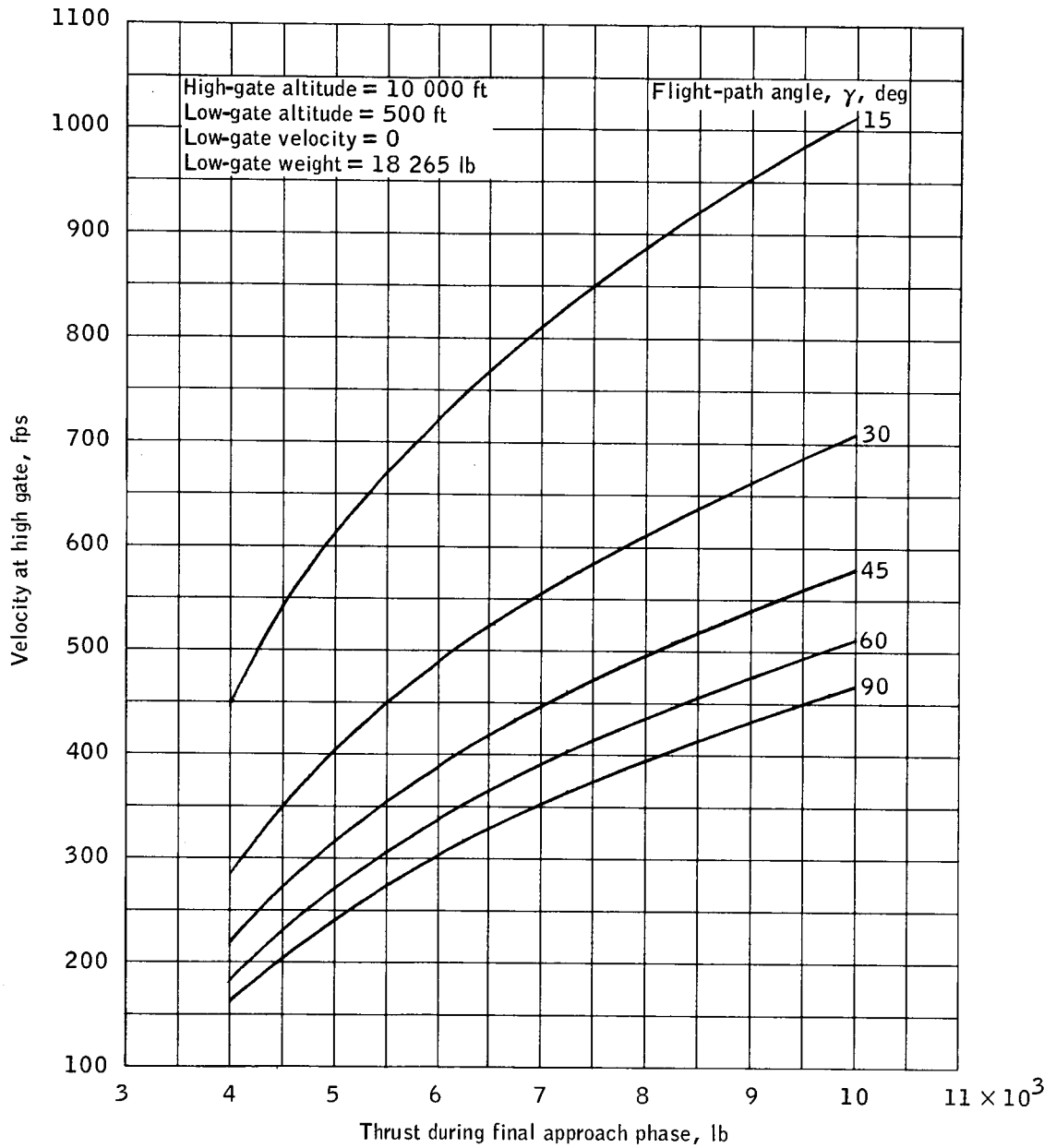

Figure 3.- Variation in the velocity at high gate with flight-path angle and thrust.

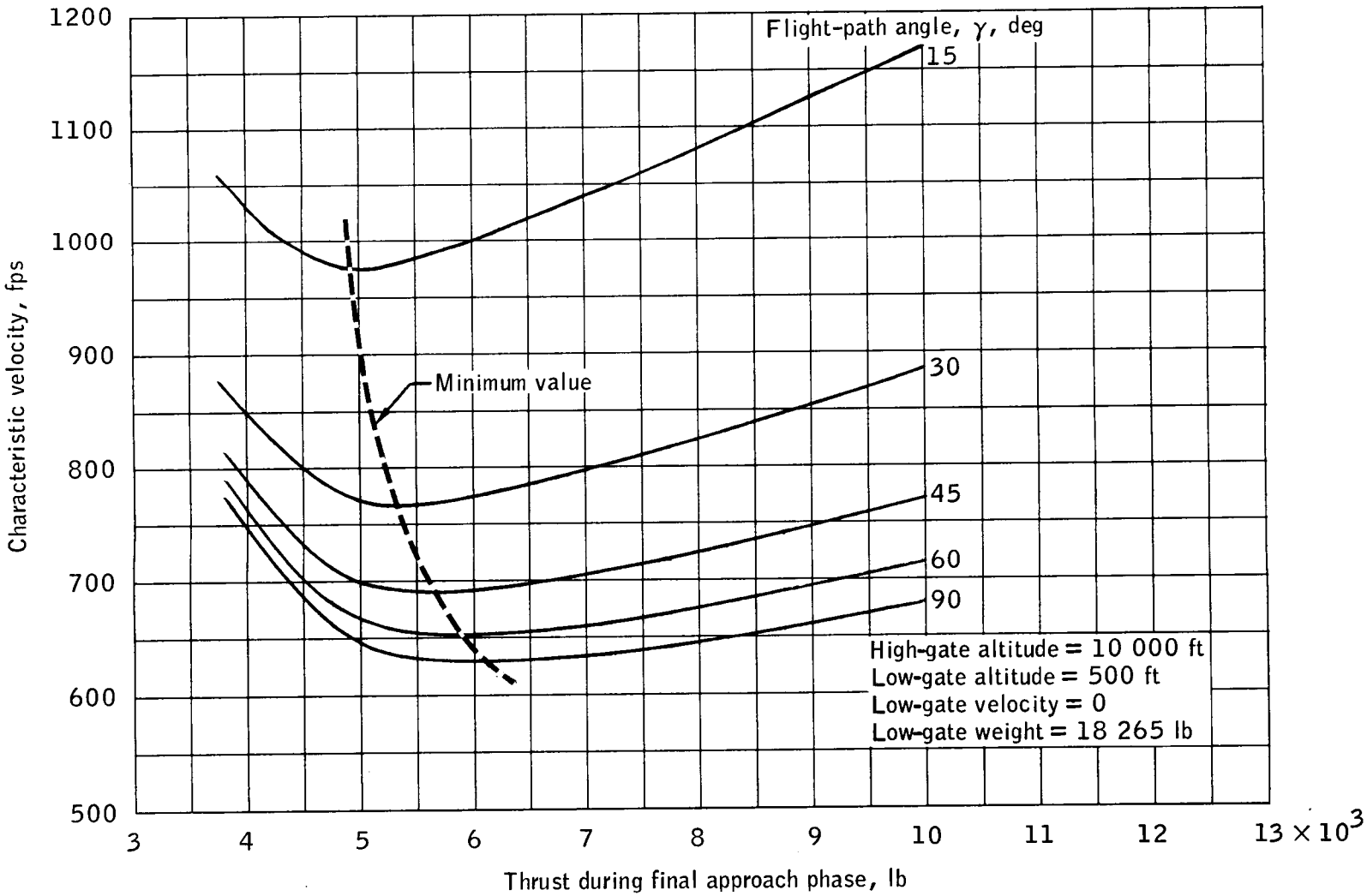

Figure 4.- Characteristic velocity required from high gate to low gate.

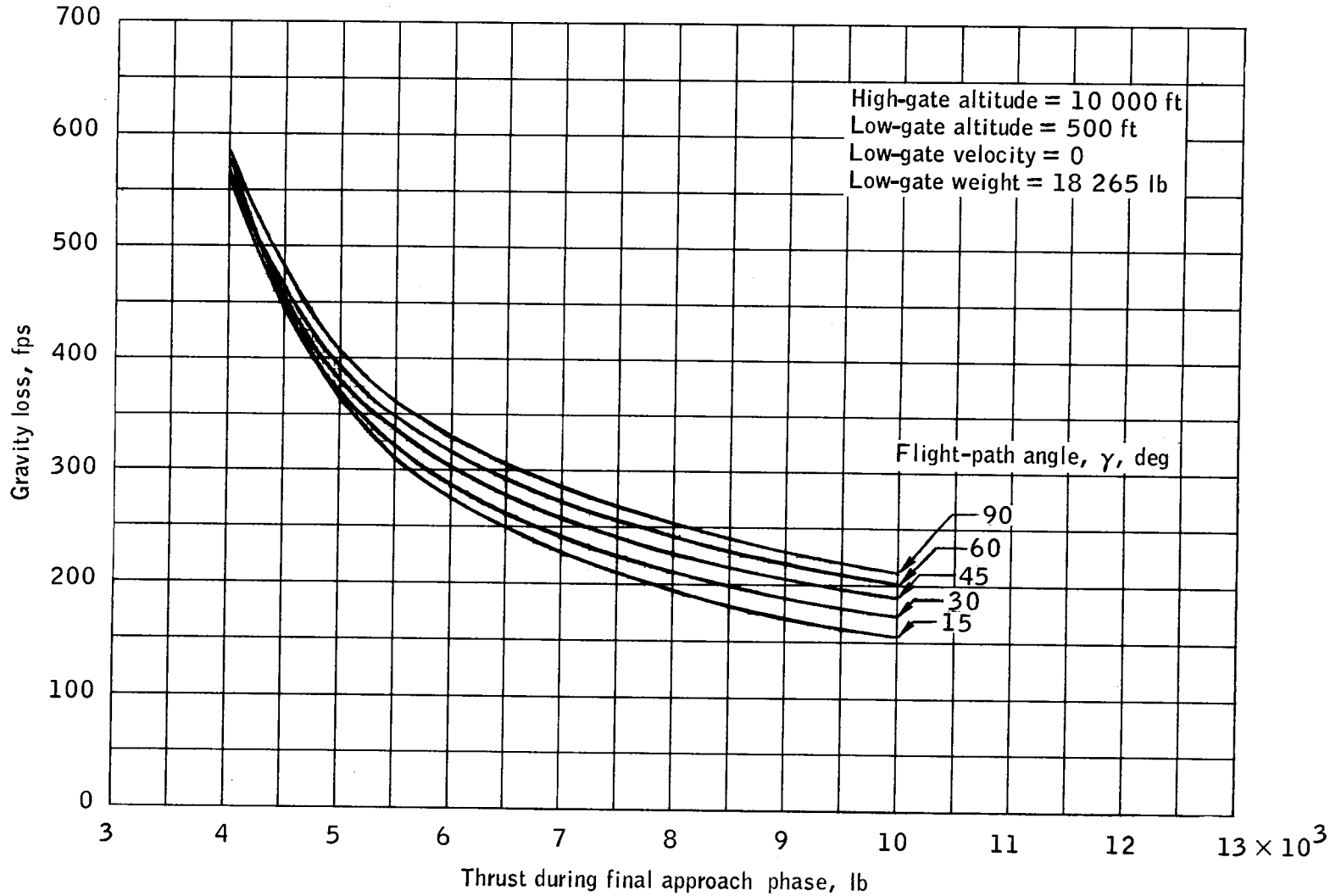

Figure 5.- Gravity losses incurred from high gate to low gate.

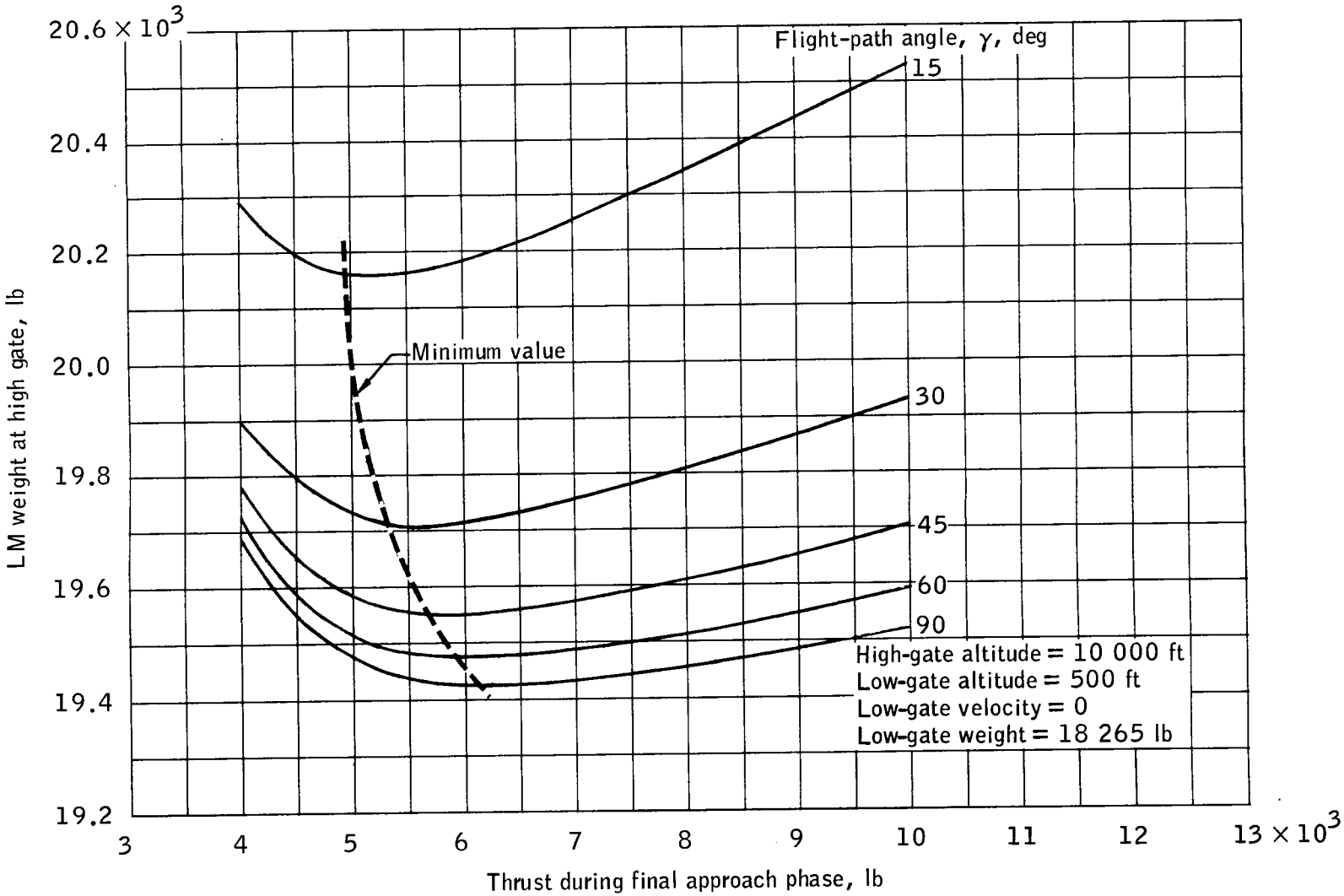

Figure 6.- Variation in LM weight at high gate with flight-path angle and thrust.

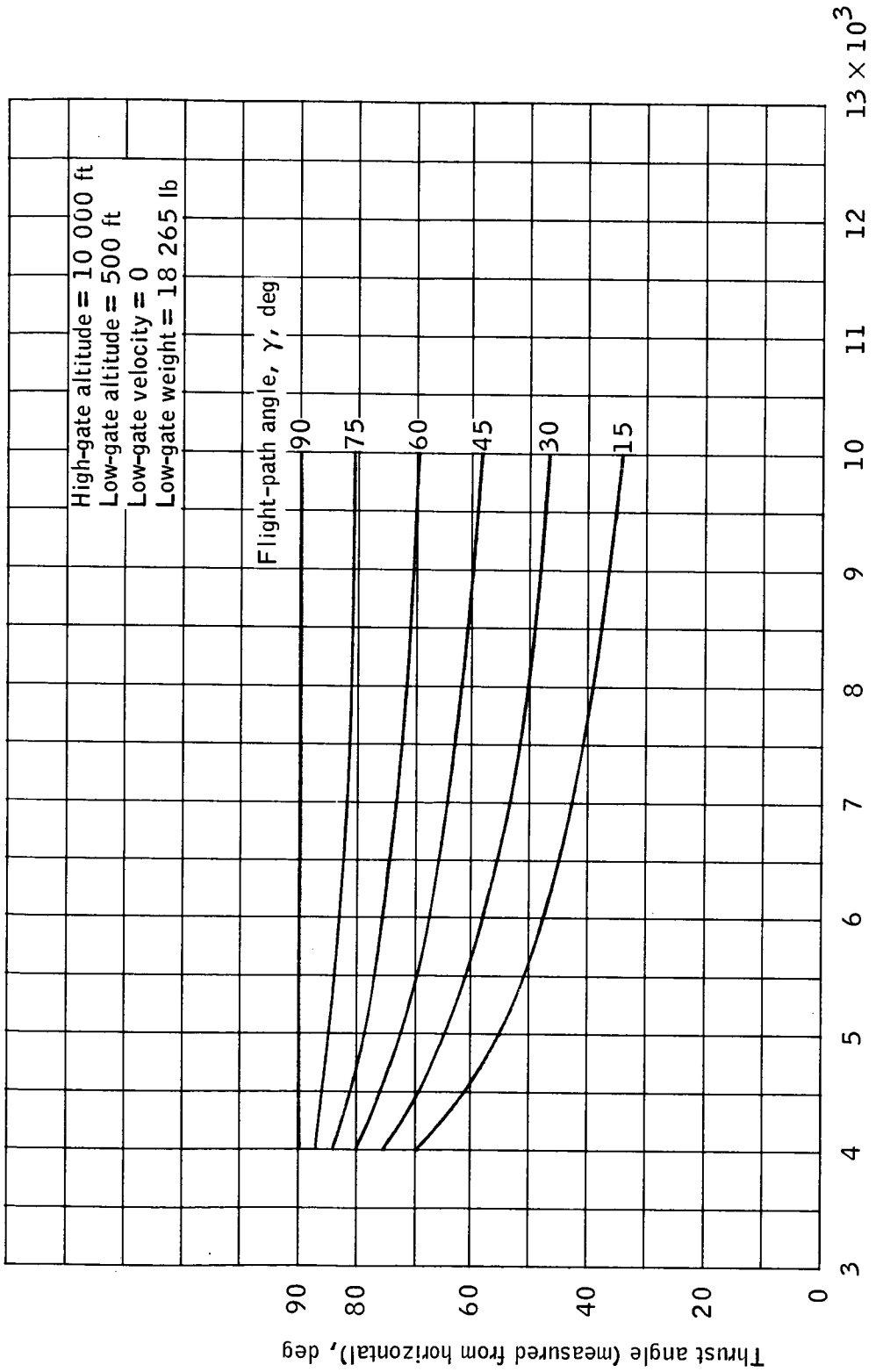

Figure 7.- Variation in thrust angle at high gate with flight-path angle and thrust.

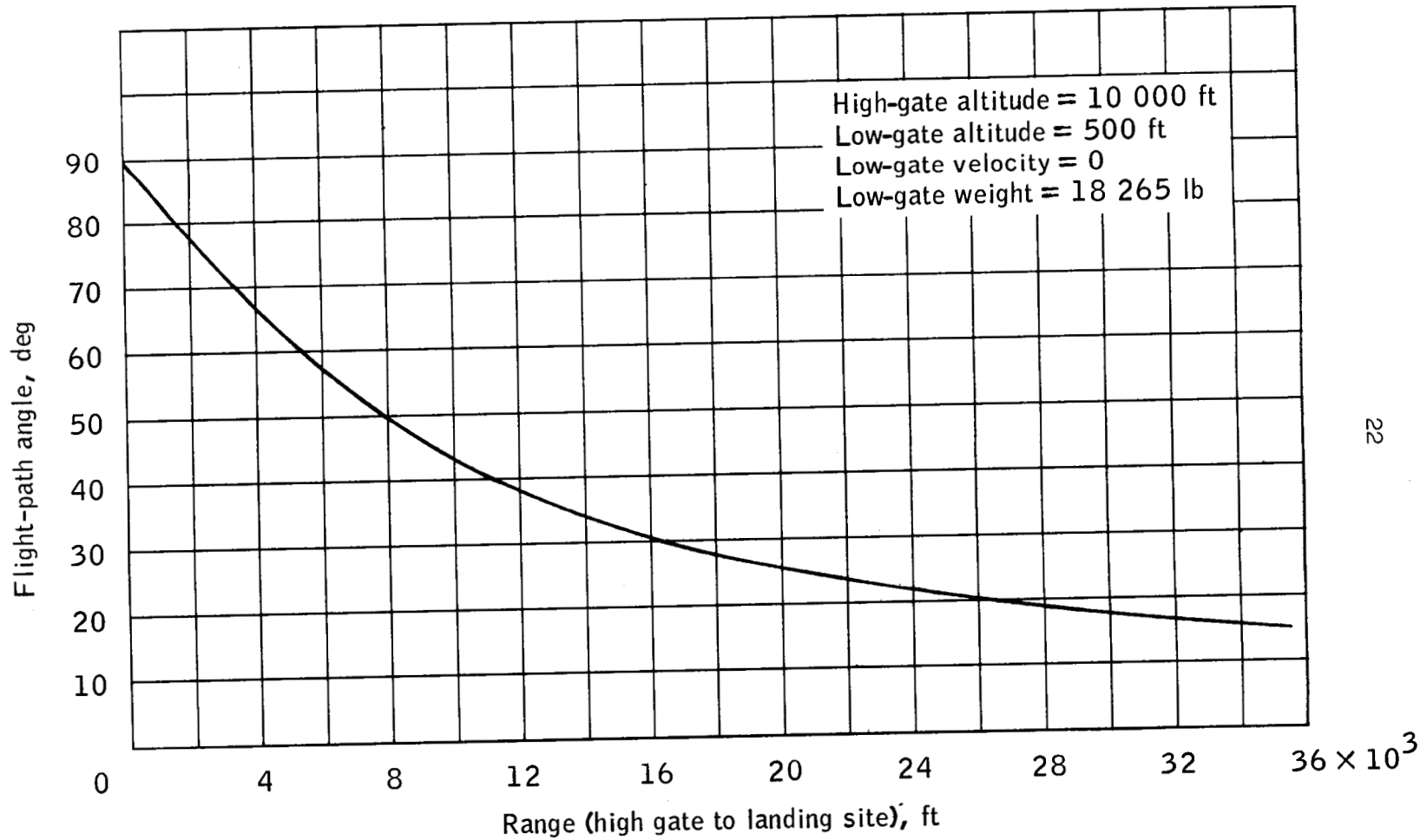

Figure 8.- Variation in ground range from high gate to landing site with flight-path angle.

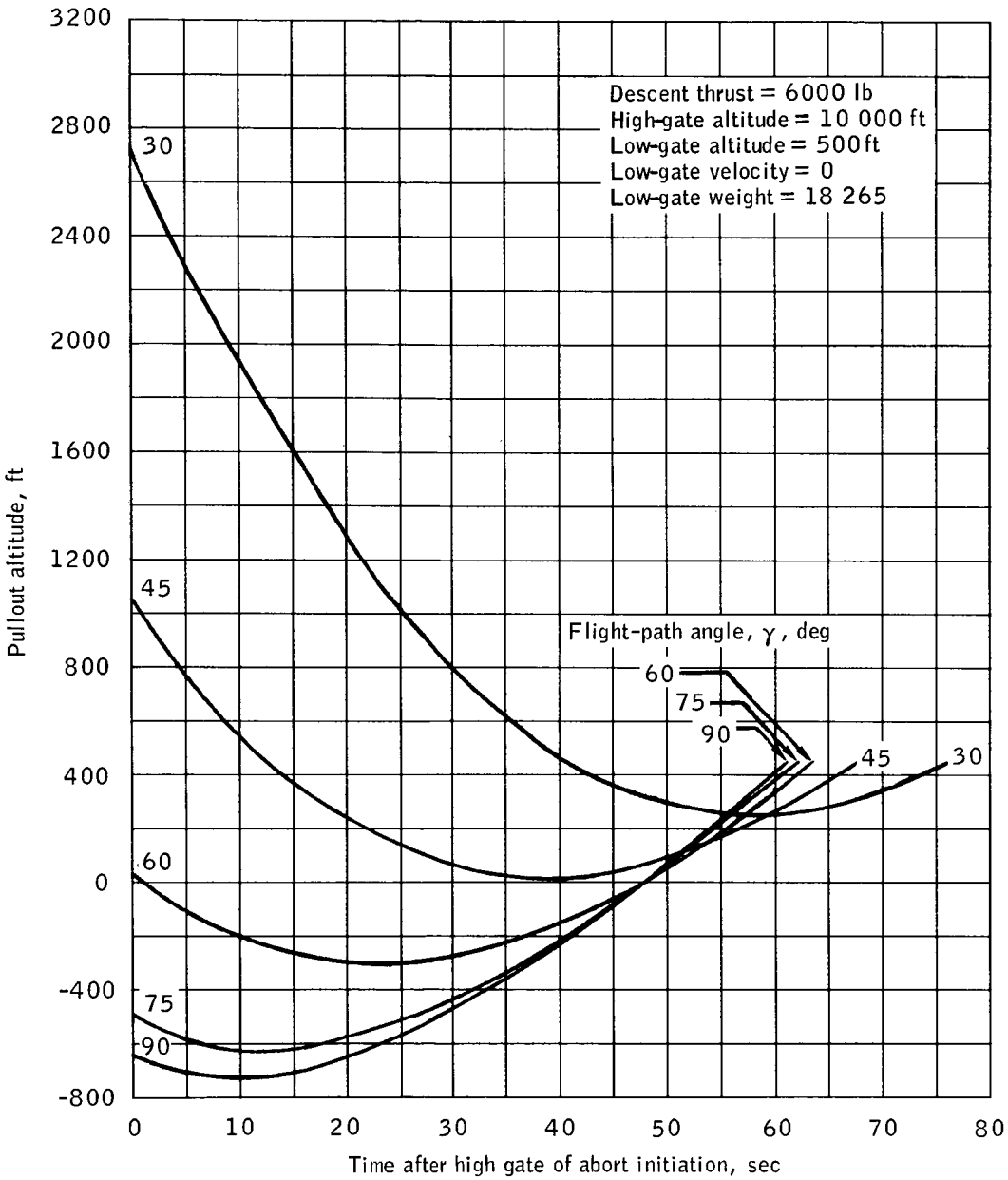

Figure 9.- Variation in pullout altitude with time of abort initiation and flight-path angle.

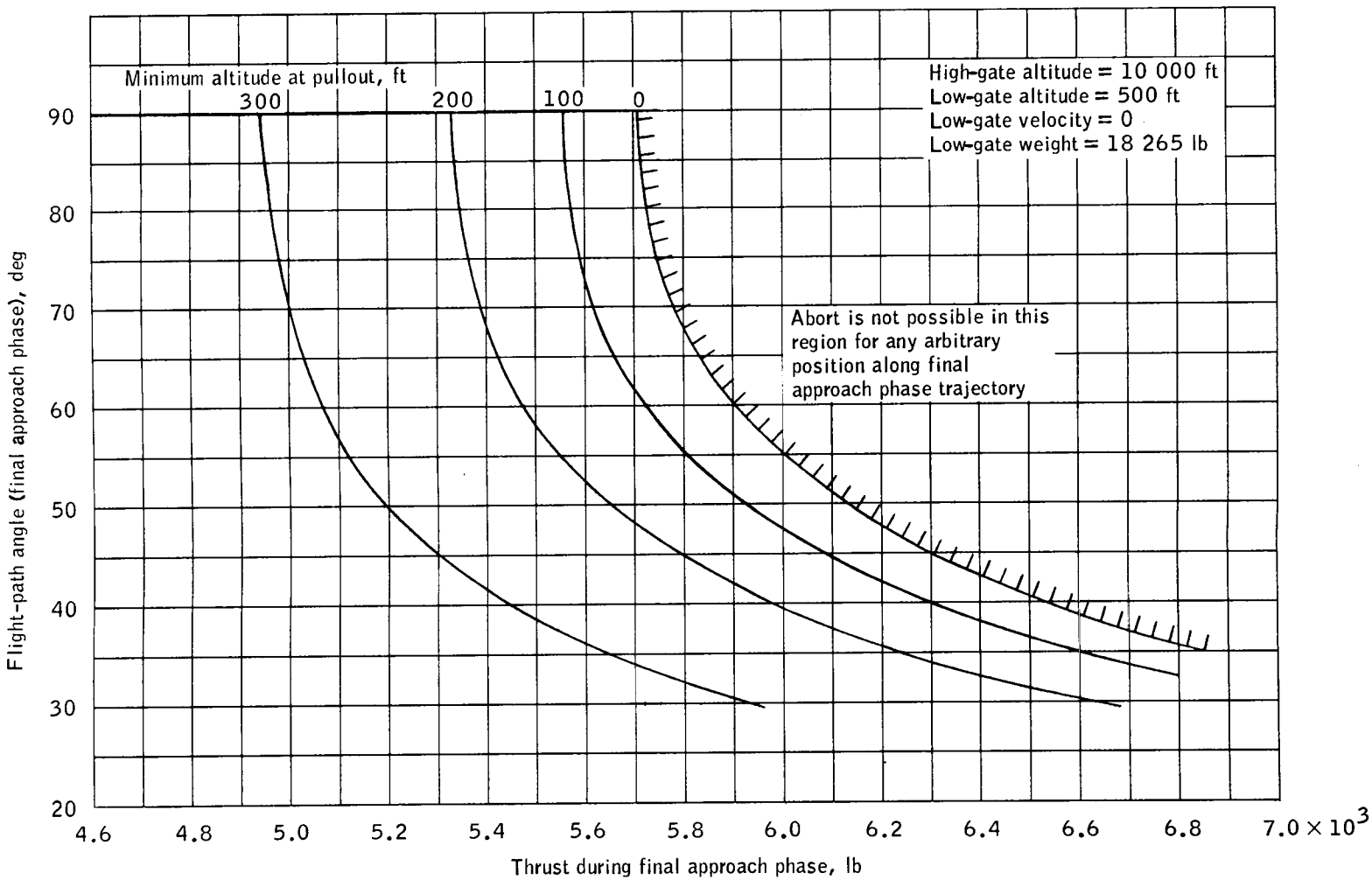

Figure 10.- Abort pullout capability of the LM ascent stage.

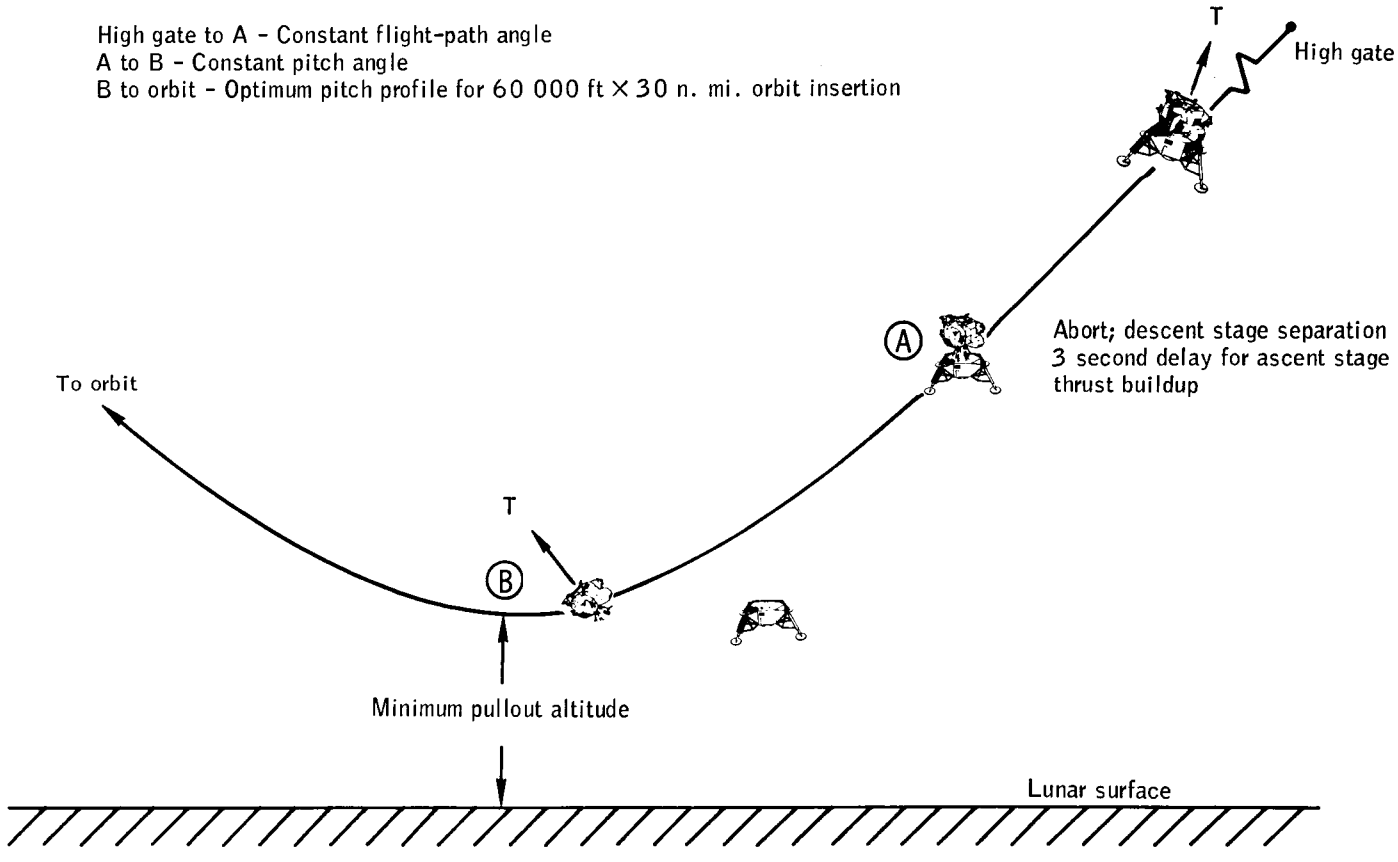

Figure 11.- Method of abort from steep descent.

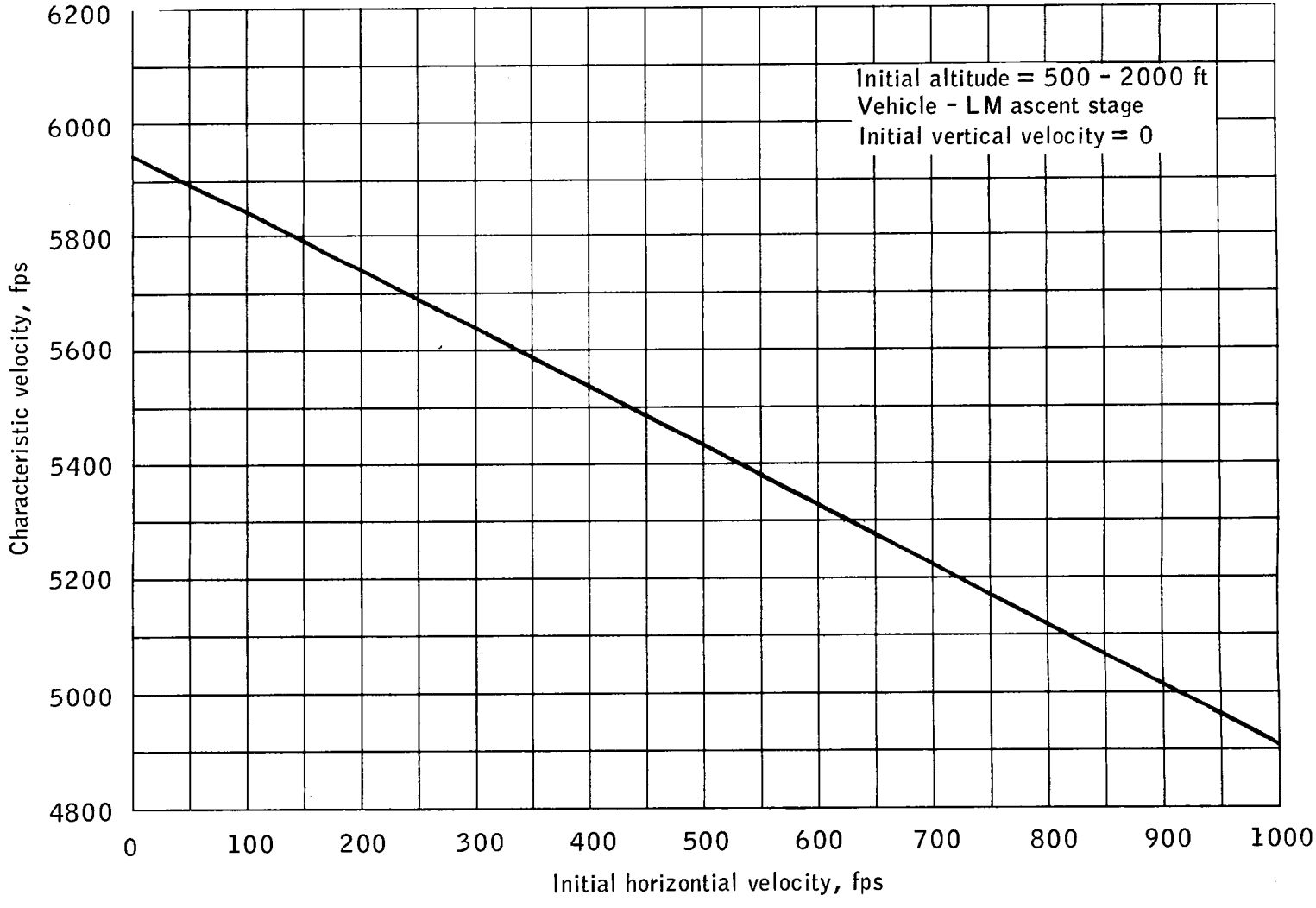

Figure 12. - Characteristic velocity required to attain 60 000-foot by 30-nautical mile orbit.

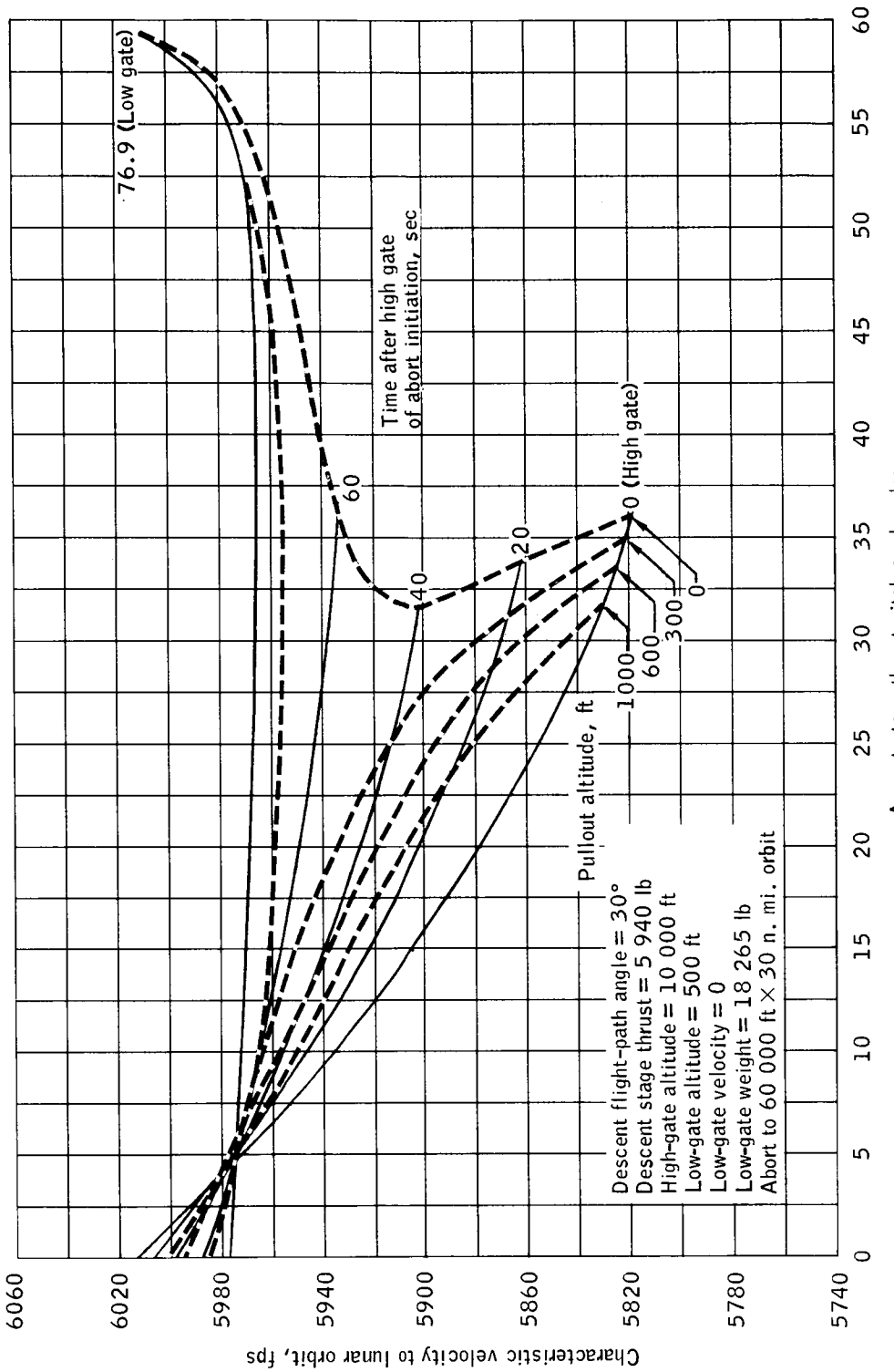

Figure 13.- Characteristic velocity required for LM abort during a 30° flight-path angle final approach phase.

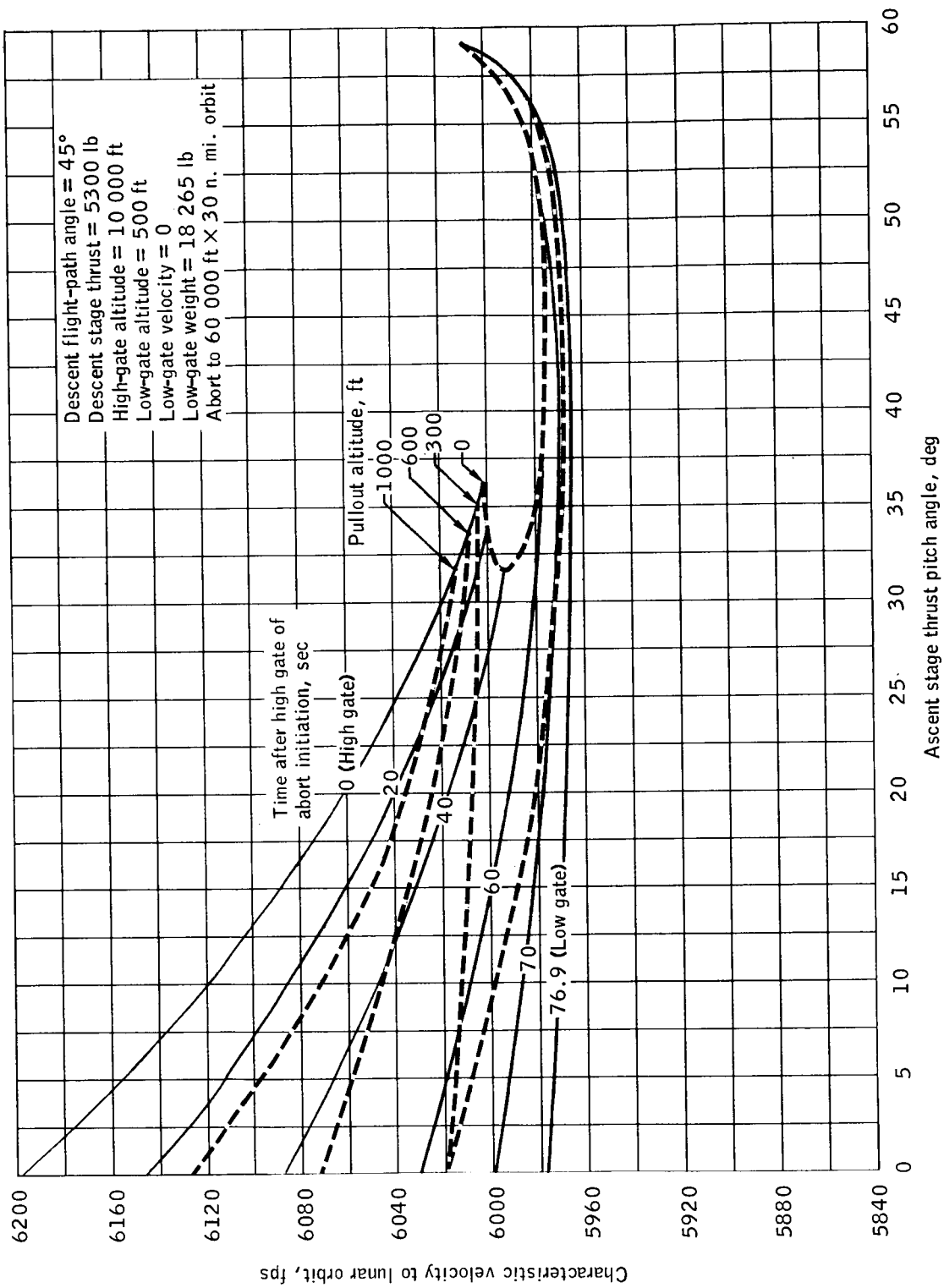

Figure 14.- Characteristic velocity required for LM abort during a 45° flight-path angle final approach phase.

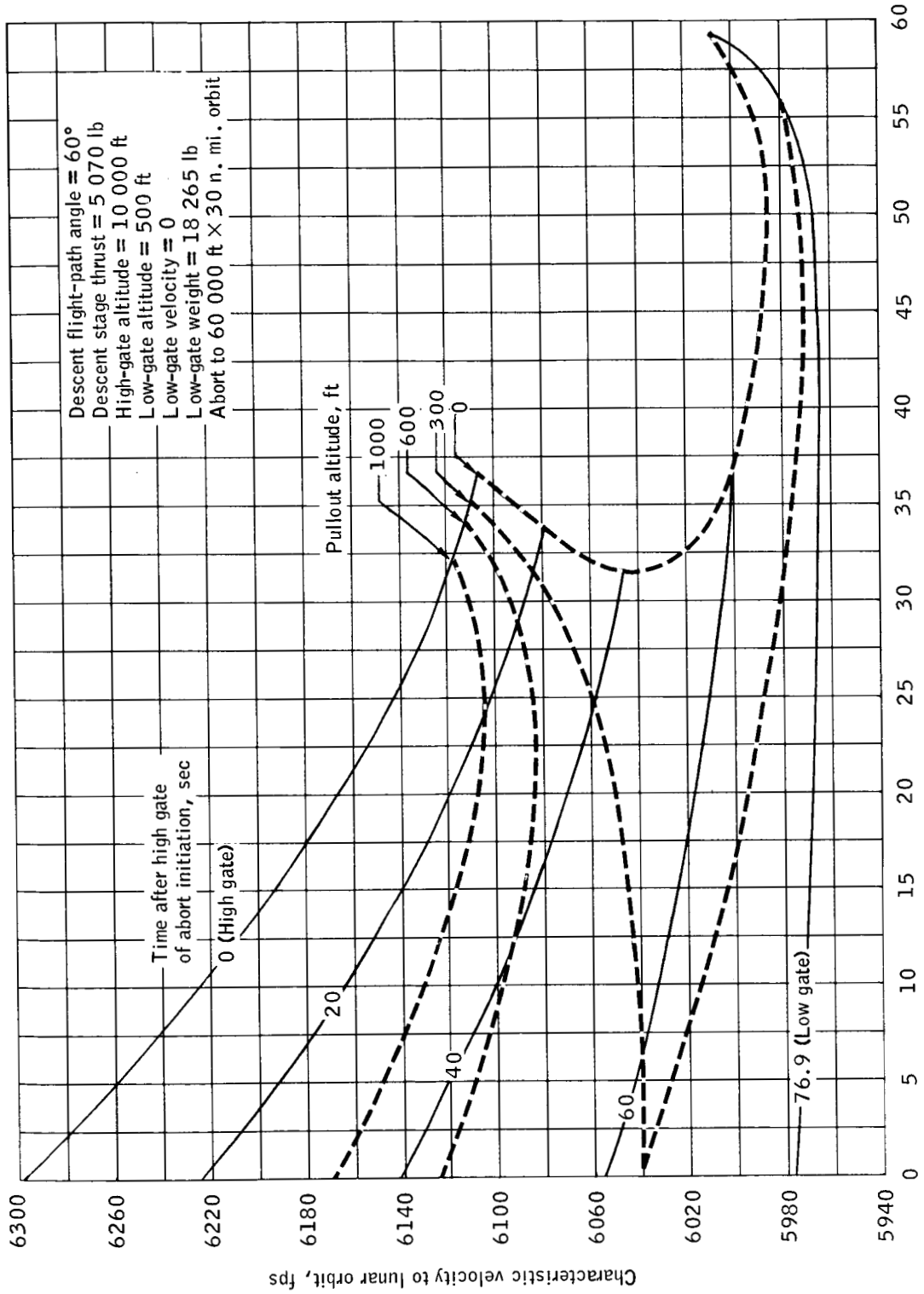

Figure 15.- Characteristic velocity required for LM abort during a 60° flight-path angle final approach phase.

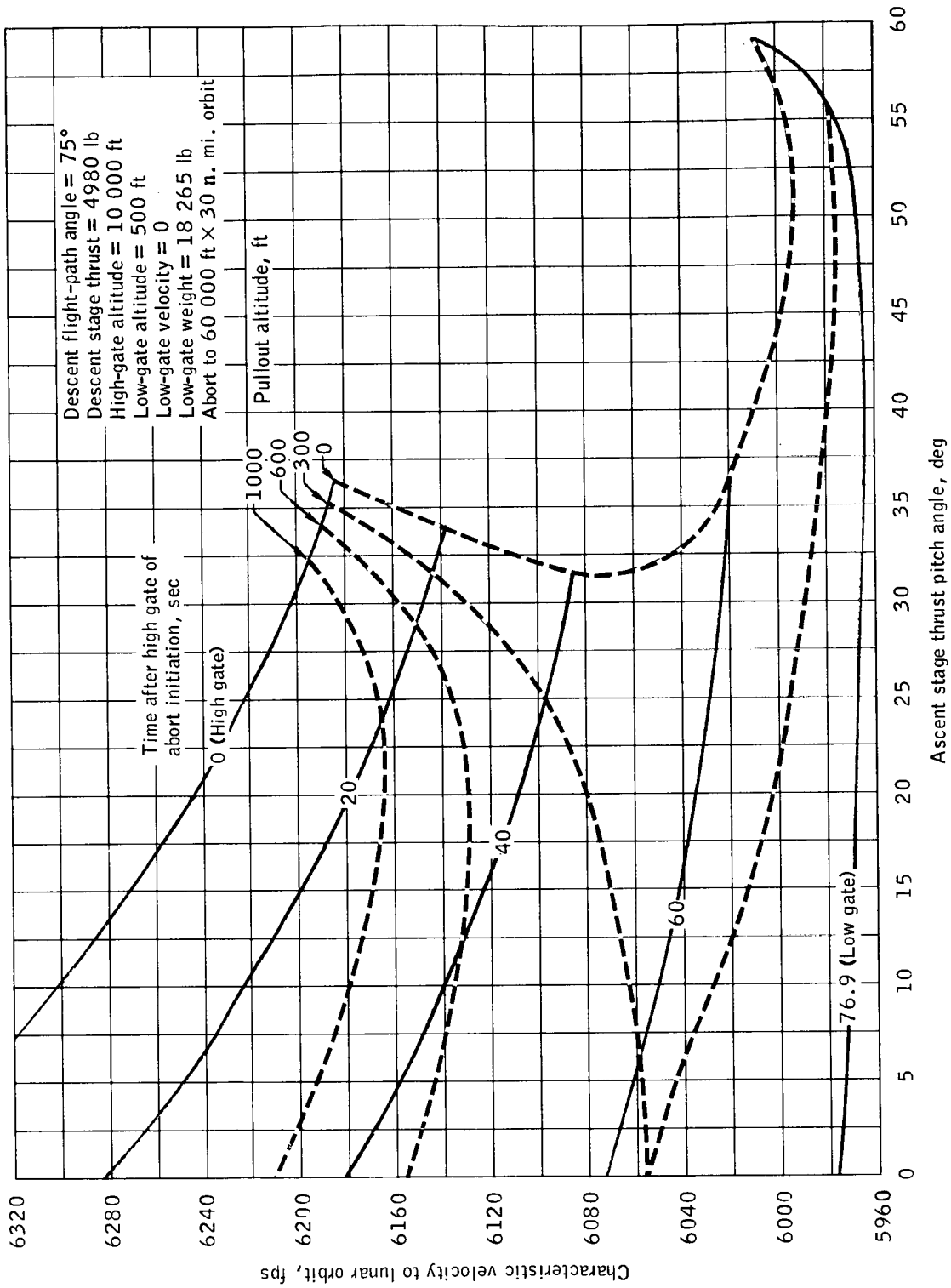

Figure 16.- Characteristic velocity required for abort during a 75° flight-path angle final approach phase.

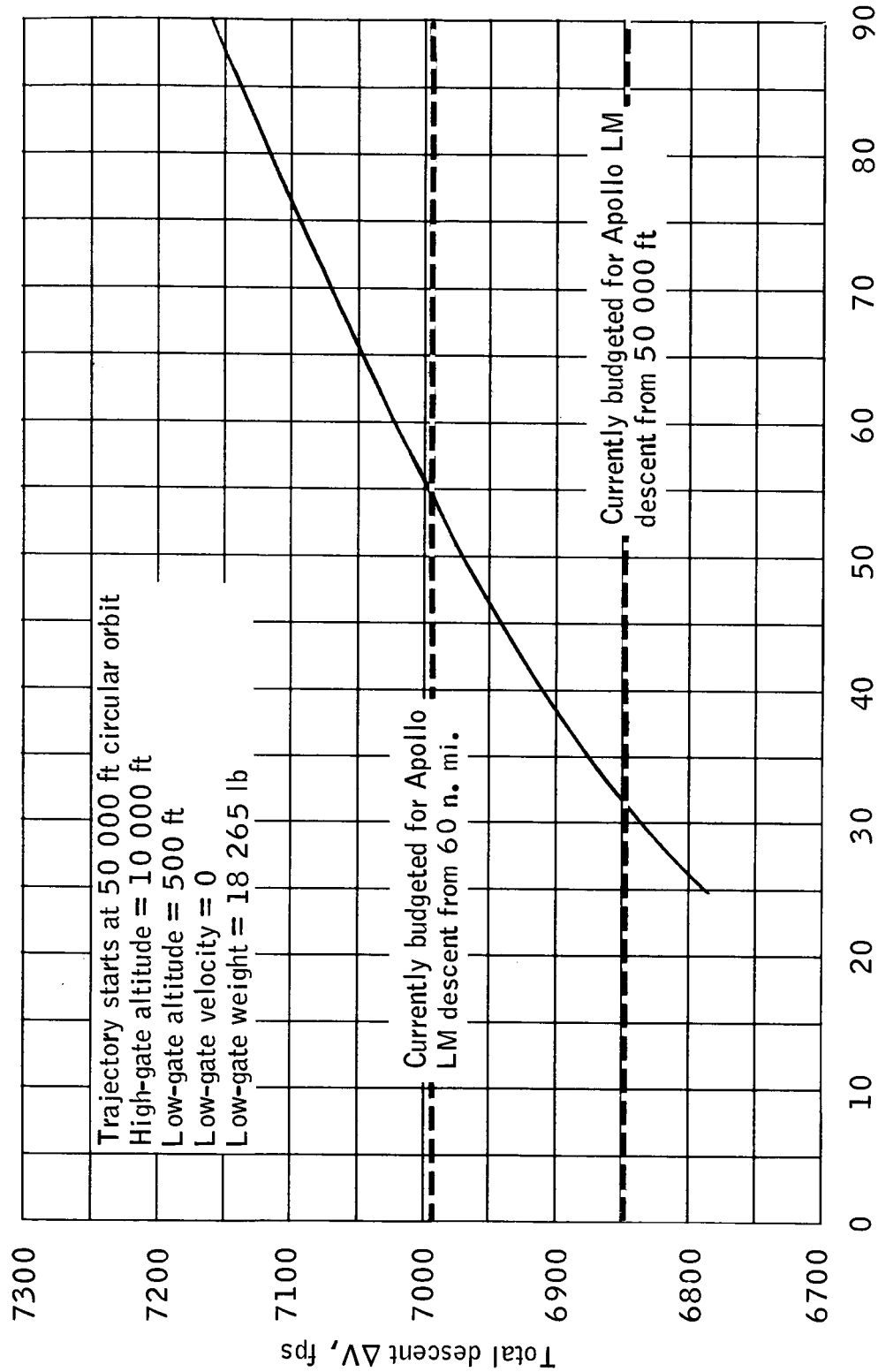

Figure 17.- Total ΔV required for LM descent using a steep final approach phase.

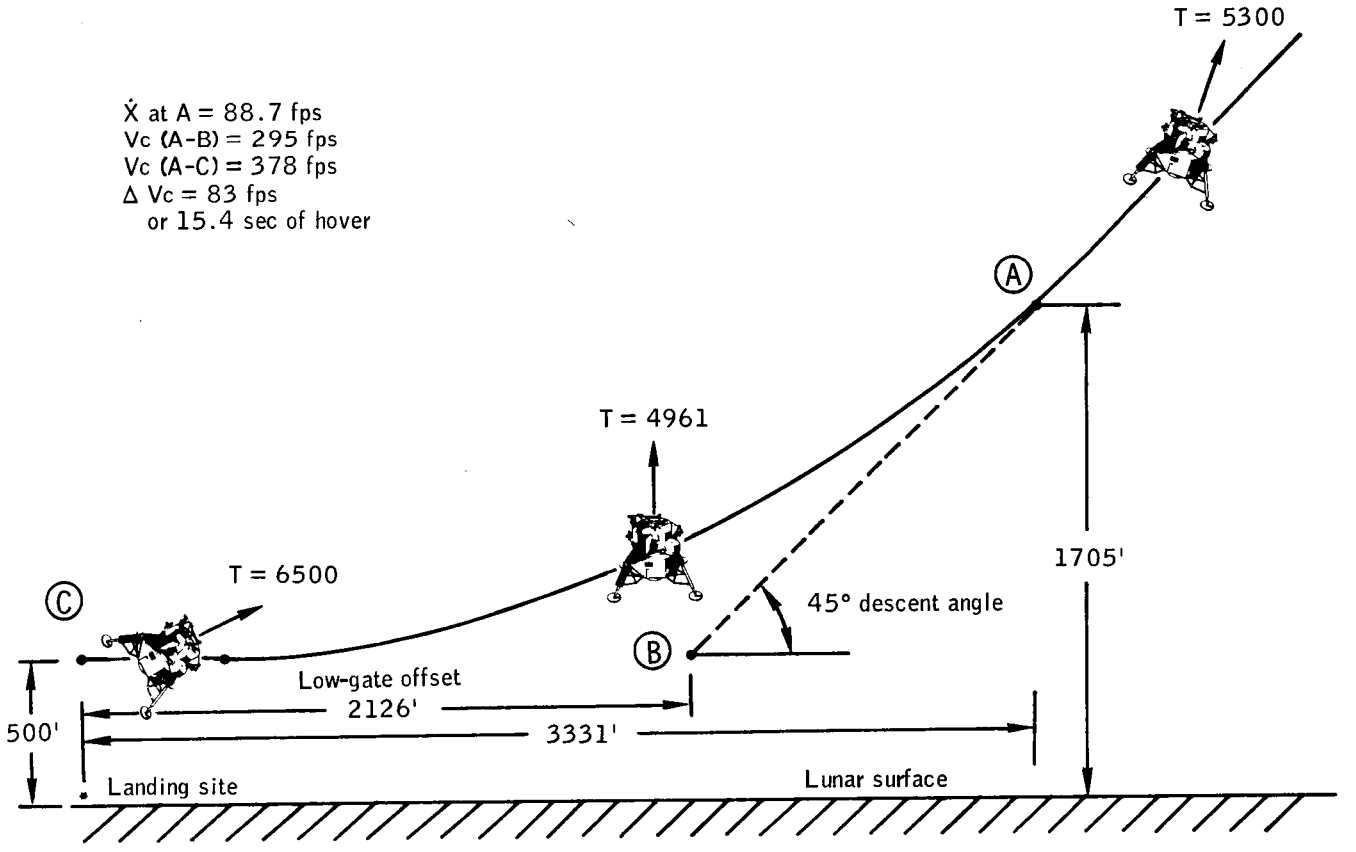

Figure 18.- Low-gate offset technique for landing site visibility.

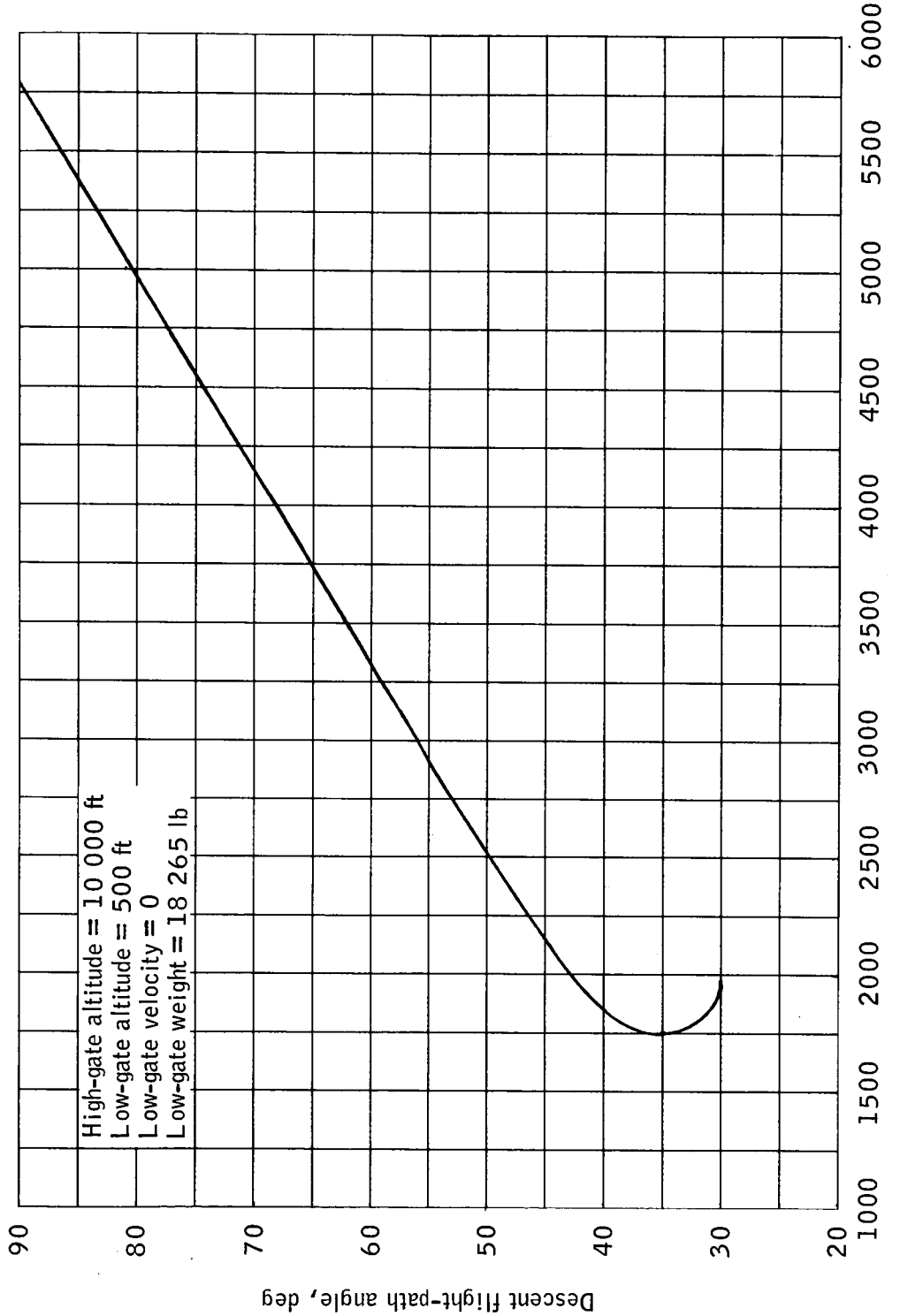

Figure 19.- Low-gate offset technique required for landing site visibility at high gate.

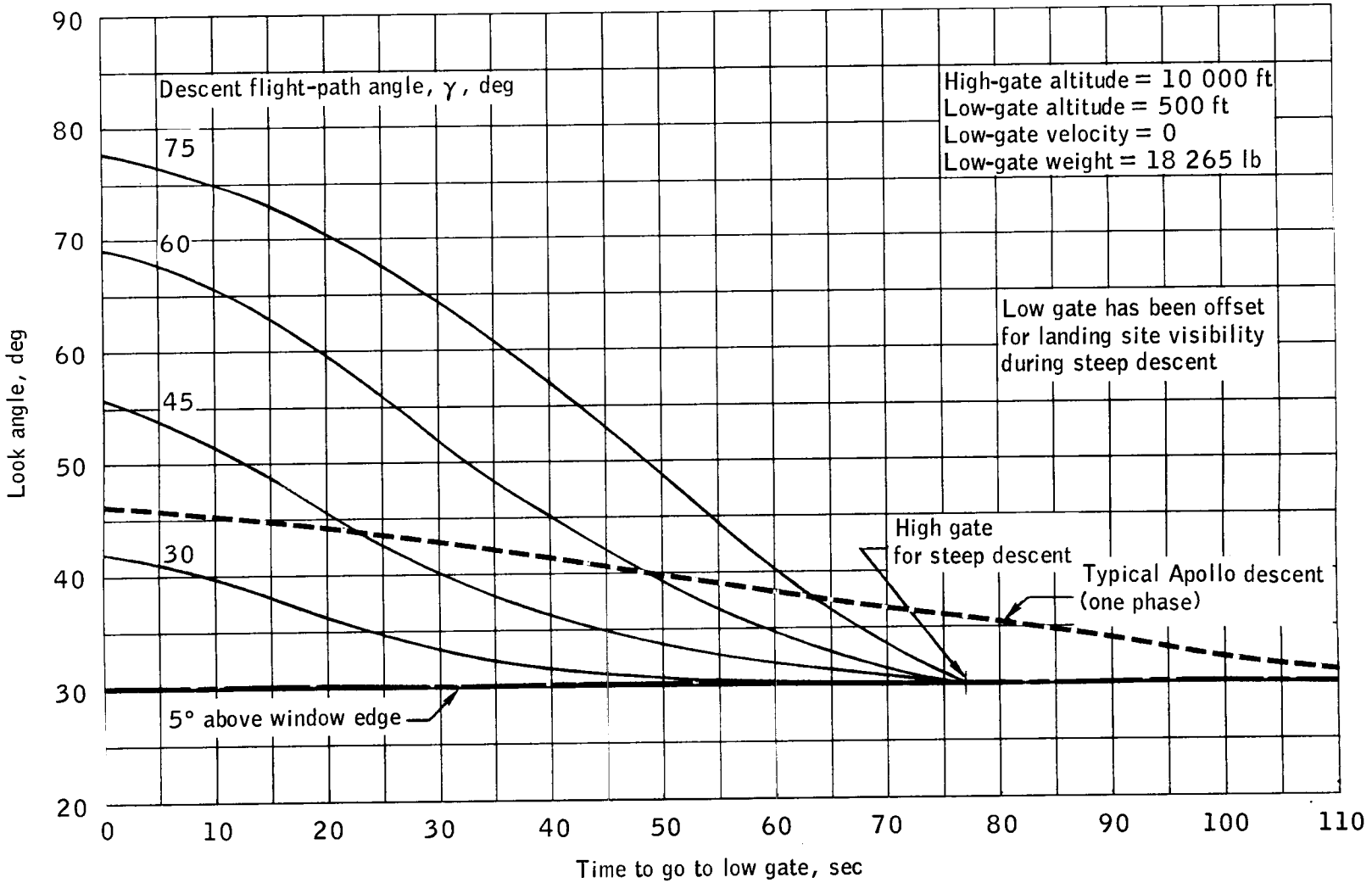

Figure 20.- Look angle with low-gate offset.

REFERENCES

1. Funk, Jack: ELM ΔV and Propellant Budget. MSC memo 68-FM8-57, June 25, 1968.

2. Taylor, B. G.: Effects of Increase in DPS Throttle Limit and I_{sp} for LM Descent. MSC memo 68-FM2-43, April 2, 1968.

3. Low, G. M.: Supplement I to Apollo Spacecraft Weight and Mission Performance Definition (December 12, 1967). July 10, 1968.

4. Lamey, W. C.: LM Abort Data for Action Item 0021-4003 (Verification of the Analytic Abort Program). MSC memo 68-FM22-154, October 2, 1968.